Theoretical investigation of cyano-chalcogen dimers and their importance in molecular recognition

Previtali, Viola; Sánchez-Sanz, Goar ; Trujillo, Cristina

Published in:
ChemPhysChem

Link to article, DOI:
10.1002/cphc.201900899

Publication date:
2019

Document Version
Peer reviewed version

A EUROPEAN JOURNAL

CHEMPHYSCHEM

OF CHEMICAL PHYSICS AND PHYSICAL CHEMISTRY

Accepted Article

Title: Theoretical investigation of cyano-chalcogen dimers and their importance in molecular recognition

Authors: Viola Previtali, Goar Sánchez-Sanz, and Cristina Trujillo

To be cited as: *ChemPhysChem* 10.1002/cphc.201900899

Link to VoR: http://dx.doi.org/10.1002/cphc.201900899

A Journal of

ChemPubSoc Europe

WILEY-VCH

www.chemphyschem.org

ARTICLE WILEY-VCH

Theoretical investigation of cyano-chalcogen dimers and their importance in molecular recognition

Viola Previtali, [a] Goar Sánchez-Sanz[b] and Cristina Trujillo,*[c]

In this manuscript the different noncovalent interactions established between $(HYCN)_2$ dimers (Y = S, Se and Te) have been studied at the MP2 and CCSD(T) level of theory. Several homodimers have been taken into account, highlighting the capacity of these compounds to act both as electron donor and acceptor. The main properties studied were geometries, binding energy (E_b), and molecular electrostatic potential (MEP). Given the wide application of chalcogen bonds, and more specifically of cyano-chalcogen moieties in molecular recognition, natural bond orbital (NBO), "atoms-in-molecules" (AIM), and electron density shift (EDS) analysis were also used to analyse the different noncovalent interactions upon complexation. The presence of hydrogen, chalcogen and dipole-dipole interactions was confirmed and their implications on molecular recognition were analysed.

Introduction

Noncovalent interactions are particular type of weak interactions that differ completely form the stronger covalent interactions, and, as their name suggest, they do not need an overlap of orbitals for them to happen, but they can originate different range of strength as van der Walls and ion-ion interaction.[1, 2]

Noncovalent interactions play a fundamental role in modern chemistry, physics and in bio-system. Besides contributing to the stability of large supramolecular and polymers[1], they can also play a fundamental role in the folding of complex biological systems.[3]

The number of weak interactions is not only limited to the classical and well known hydrogen bond (HB)[4-7] but other kind of noncovalent interactions are halogen bonds[8-12], hydride bonds[13, 14], tetrels[15-19], chalcogen[20-25] and pnicogen (or pnictogen) interactions. [2, 26-36]

The nature of the halogen bond is explained by attractive electrostatic interactions between the positive σ-hole on the halogen atom and negative charge of the donor (Lewis Base).[37-39] Similarly chalcogen atoms (O, S, Se, Te and Po) can form noncovalent complexes with electron donors, known as chalcogen bonding (ChB).[40, 41]

Like hydrogen and halogen bonding, chalcogen bonding plays an important role in the synthesis, catalysis, and design of materials[42, 43], but also in the functionality of biological systems. No bonded interactions between a divalent sulphur atom and polar functional groups, i.e., S···X (X = O, N, and S) interactions, have recently been demonstrated to stabilize protein structures.[44] It has lately been demonstrated that chalcogen bonds have important roles in protein-ligand complexes and innovative approaches try to exploit these molecular recognition features in drug design.[45-47]

The increasing number of nitrile-containing pharmaceuticals, makes the cyano group a very interesting and worth studying moiety with applications in drug design and molecular recognition.[48-50] Nitriles are unusual and versatile functionalities, and these features are often related to their short and polarized triple bond.[51] In some cases the strong dipole can facilitate polar interactions in which the nitrile acts as a hydroxyl or carboxyl isostere, in other cases nitrile play key roles as hydrogen bond acceptor.[48] It has also been demonstrated that, when the nitrile group is activated by adjacent withdrawing group, it behaves as an electrophile towards nucleophiles as cysteine.[52]

Sulphur containing functional group can be found in a wide range of pharmaceutical, and besides nitrogen and oxygen, sulphur maintains its dominating heteroatom role in FDA approved drugs.[53] Thiocyanate (SCN) is an important molecule with the potential to establish molecular recognition with the host environment and foreign organisms and to act as both host defence and antioxidant agent, making it a potential useful therapeutic.[54, 55] Thiocyanate-containing natural products have been isolated and studied for their biological activity[56] and the thiocyanate moiety has been inserted into potential anticancer agents[57] and inhibitors of the protozoan *Trypanosoma cruzi*.[58, 59] Additionally, the recent applications of organic thiocyanate in drug development has also let to recent advances to their chemistry and accessibility.[60]

Similarly, selenium plays an important role in normal biological function[61] through its incorporation into processes that protect against oxidative stress, and its bioactivity mechanism has been studied using DFT calculations.[62] Selenocyanate-containing derivatives have been found to possess anticancer and chemopreventive[63-65], antifungal[66], and antileishmanial[67, 68] activity. Therefore, their synthesis, characterization, and uses in chemistry and molecular recognition have recently gained a lot of interest.[69-72]

[a] Center for Nanomedicine & Theranostics, Department of Chemistry, Technical University of Denmark, Kemitorvet 207, Kongens Lyngby, DK, Denmark
[b] Irish Centre of High-End Computing, Grand Canal Quay, Dublin 2, Ireland & School of Chemistry, University College Dublin, Belfield, Dublin 4, Ireland
[c] School of Chemistry Trinity Biomedical Sciences Institute, Trinity College Dublin 152-160 Pearse Street, Dublin 2, Ireland
*Corresponding authors: trujillc@tcd.ie, +35318964229

Electronic Supplementary Information (ESI) available: [experimental procedures and characterisation data]. See DOI:

The application of chalcogen bonding in molecular recognition has also been employed in the selective separation of isomeric mixtures, where the receptors consist of bifurcated chalcogen bond donor centres (sulphur or selenium) towards the cyano group nitrogens of neighbouring molecules.[42, 73] In addition, due to their application in crystal engineering, the structures and properties of chalcogens dicyanide in crystalline complexes[74] or in ChB with hydrogen cyanide (HCN) were recently studied.[75-77] Finally, chalcogen bond donors are reported to interact with halides, and a single example involving NC-Se-Se-CN has also been reported paving the way as possible anion receptors in molecular recognition[78].

Compared to sulphur and selenium the incorporation of tellurium in bioactive molecules is still at its infancy. However, the recently progresses made have been responsible for the increased attention towards tellurium and its applications in chemistry, material science but also drug discovery.[41, 79-81]

Following this research line and given the wide applications that the incorporations of chalcogen as sulphur, selenium, tellurium, and, in particular, their cyanates derivatives, have on chemical and biochemical sceneries, we herein describe a computational study of cyano-chalcogen homodimer derivatives (**Figure 1**). We have therefore the aim of improving the knowledge of the theoretical behaviour of the corresponding monomers by characterization of bonds types established and cooperativity between interactions, with the hope of improving their understanding for future application and design in molecular recognition.

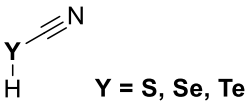

Y = S, Se, Te

Figure 1. Schematic representation of the cyano-chalcogen monomers under study.

Results and Discussion

Monomers

We began by calculating the molecular electrostatic potential (MEP) surfaces for the three monomers to analyse the areas susceptible of nucleophilic and electrophilic attacks. Maxima and minima values of the MEP on the 0.001 a.u. electron density isosurface which resembles to the van der Waals surface (vdW) were plotted in **Figure 2** and summarised in **Table 1**.

Two MEP minima values (black dots) were found for the chalcogen atom, one corresponding to the lone pair associated to the N atom ($V_{min,N}$) and another one corresponding to the chalcogen lone pairs ($V_{min,Y}$). While the former is negative the latter has been found to be slightly positive. In term of maxima values, three critical points on the surface were located. One, $V_{max,H}$, corresponding to the hydrogen, second one, $V_{max,YH}$, a S σ-hole on the Y-H bond axis and finally the σ-hole on the Y-CN axis, $V_{max,YCN}$, which exhibits the deepest σ-hole of the monomers.

As observed, $V_{min,N}$ value decreases with the size of the chalcogen, while the depth of $V_{max,YCN}$ increases. The largest one of the three (0.7436 au) is found in **TeCN**, in agreement with the polarizability of the atom. So, in principle, one should expect that the interaction head-to-tail, N···Y, will increase with the size of the chalcogen.

Table 1. Maxima ($V_{max,x}$) and minima ($V_{min,x}$) values of the molecular electrostatic potential (in a.u.) over the 0.001 e^- electron density isosurface for all the monomers calculated at MP2/aug-cc-pVTZ level.

	$V_{min,N}$	$V_{min,Y}$	$V_{max,YCN}$	$V_{max,YH}$	$V_{max,H}$
HSCN	-0.0536	0.0008	0.0617	0.0403	0.0690
HSeCN	-0.0542	0.0005	0.0656	0.0448	0.0587
HTeCN	-0.0559	0.0004	0.0744	0.0523	0.0432

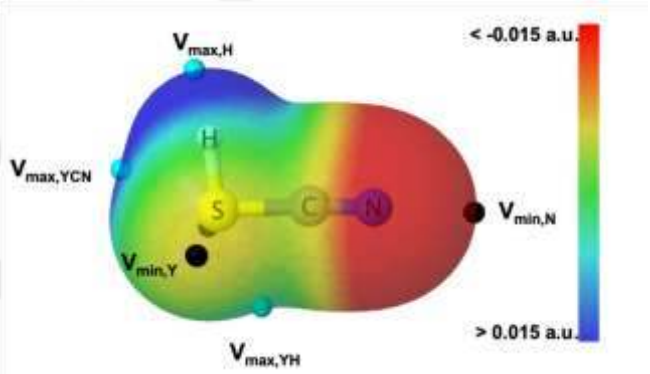

Figure 2. Molecular electrostatic potential on the 0.001 e^- electron density isosurface for **HSCN** monomer. Maxima and minima values of MEP are represented by cyan and black dots, respectively.

The structure of the three different **HYCN** isolated monomers has been optimised and their structural parameters reported in **Table 2**. Data calculated for the C-Y bonds are in good agreement with those reported in the literature, with the largest deviation found for C-Se. C-N bonds are in very good agreement with the experimental data found.

Table 2: Structural data for the **HYCN** monomers at the MP2/aug-cc-pVTZ computational level.

		HSCN	HSeCN	HTeCN
***d*(C-Y) [Å]**	**Exp.**	1.47 –1.69[a]; 1.701[b]	2.01 - 2.08[c]	2.090 - 2.091[d]
	Theor.	1.697	1.828	2.032
***d*(C-N) [Å]**	**Exp.**	1.17–1.33[a]; 1.156[b]	1.07 - 1.27[c]	1.131 - 1.149[d]
	Theor.	1.175	1.175	1.176
***d*(Y-H) [Å]**	**Exp.**	1.55[a]	-	-
	Theor.	1.340	1.454	1.644

[a] *Beard, C. I. and B. P. Dailey. "The Structure and Dipole Moment of Isothiocyanic Acid." Journal of Chemical Physics 18, no. 11 (1950): 1437-1441.*
[b] *Refers to $S(CN)_2$: Pierce, L., R. Nelson and C. Thomas. "Microwave and Infrared Spectra of Sulfur Dicyanide - Molecular Structure Dipole Moment Quadrupole*

Coupling Constants Centrifugal Distortion Constants and Vibrational Assignment." Journal of Chemical Physics 43, no. 10P1 (1965): 3423

[c] *Refers to Se(CN)$_2$: Linke, K. H. and F. Lemmer. "Rontgenographische Kristallstrukturanalyse Von Selendicyanid." Zeitschrift Fur Anorganische Und Allgemeine Chemie 345, no. 3-4 (1966): 211*

[d] *Refers to Te(CN)$_2$:Klapotke, T. M., B. Krumm, J. C. Galvez-Ruiz, H. Noth and I. Schwab. "Experimental and Theoretical Studies of Homoleptic Tellurium Cyanides Te(Cn)(X): Crystal Structure of Te(Cn)(2)." European Journal of Inorganic Chemistry, no. 24 (2004): 4764-4769.*

Dimers

Energy and structure

We have found 20 minima in total, 7 for both Se and Te complexes and 6 for S complexes instead. Geometries obtained for (**HSeCN**)$_2$ dimers are depicted in **Figure 3** for illustration purposes while the rest (S and Te dimers) have been included in the ESI (Table S1).

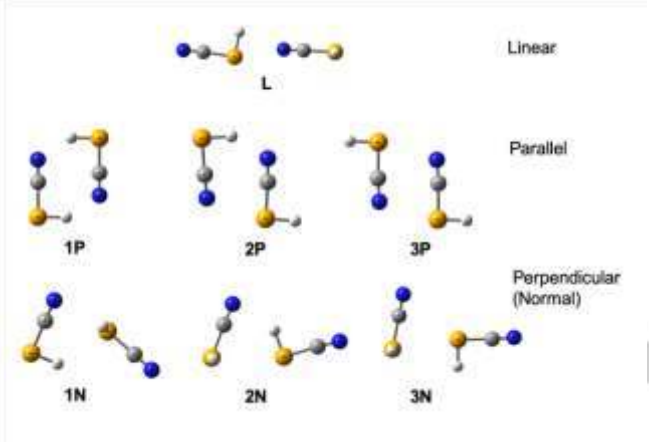

Figure 3. Optimised dimers for selenium derivatives (**HSeCN**)$_2$at the MP2/aug-cc-pVTZ computational level.

Three types of dimers were found and categorised in terms of their geometrical disposition: 1) both monomers are aligned and head to tail interaction is found, **Y$_L$**; 2) both monomers present their Y-CN bond axis in parallel, **Y$_{nP}$**; and 3) monomers present their Y-CN bond axis perpendicular one to each other, **Y$_{nN}$**. **Y$_L$** dimers show a single chalcogen interaction through the Y σ-hole. **Y$_{nP}$** complexes present more diverse type of interactions: **Y$_{1P}$** exhibit two simultaneous HB interactions and π donation, **Y$_{2P}$** one HB and π donation as well and **Y$_{3P}$** present two synchronous π donations. The latter was already described for (HXPCN)$_2$ complexes, where X is F and Cl.[82] In case of **Y$_{nN}$** dimers: **Y$_{1N}$** and **Y$_{2N}$** have one HB and presumably one ChB simultaneously while in **Y$_{3N}$** only one ChB seems to be found.

The binding energies, E_b, for all the complexes are summed up in **Table 3**. In general, when comparison of the binding energies across the chalcogen atoms is made, it is observed that tellurium derivatives present the strongest binding energy values with just one exception (**Se$_{1P}$**).

Table 3. Binding energies, E_b (in kJ/mol) for all the dimers at the CCSD(T)/CBS computational level.

(HSCN)$_2$	E_b	(HSeCN)$_2$	E_b	(HTeCN)$_2$	E_b
S$_L$	-19.2	**Se$_L$**	-24.9	**Te$_L$**	-36.8
S$_{1P}$	-42.1	**Se$_{1P}$**	-44.3	**Te$_{1P}$**	-43.0
S$_{2P}$	-30.5	**Se$_{2P}$**	-36.0	**Te$_{2P}$**	-43.7
S$_{3P}$	-19.7	**Se$_{3P}$**	-27.9	**Te$_{3P}$**	-42.4
S$_{1N}$	-16.2	**Se$_{1N}$**	-21.3	**Te$_{1N}$**	-29.1
S$_{2N}$	-	**Se$_{2N}$**	-15.9	**Te$_{2N}$**	-21.7
S$_{3N}$	-5.8	**Se$_{3N}$**	-11.1	**Te$_{3N}$**	-20.0

For the **HSCN** complexes, the overall strongest E_b (-42.1 kJ/mol) belongs to **S$_{1P}$**, where two hydrogen bonds are responsible for the stability of the complex, while **S$_{3N}$** is the weakest dimer (-5.8 kJ/mol). Chalcogen intermolecular interactions found in **S$_L$** and **S$_{nN}$** dimers are not competitive with the dipole-dipole (μ-μ) interactions and HB found for **S$_{nP}$** complexes. But does it also happen when the chalcogen atom is more polarizable? Can those ChBs for Se and Te derivatives be competitive and eventually stronger than the HB or the μ-μ interactions?

Looking at the selenium cyanide dimers, the interaction energy calculated for the dimer **Se$_L$** is 5.7 kJ/mol stronger than its sulphur-homologous **S$_L$**, evidencing the increasing of the polarizability of the chalcogen atom from S to Se, and also in alignment with the increasing found in the corresponding σ-hole (from 0.0617 to 0.0656 a.u. for **HSCN** and **HSeCN** respectively, **Table 1**). This behaviour is also observed in **Se$_{nN}$** complexes, where an increasing of the strength of the interaction (more negative E_b) is found. However, **Se$_{1P}$** dimer, in which two intermolecular HBs are located, is still the most stable complex in terms of E_b (-44.3 kJ/mol). But, while the E_b difference between the chalcogen bonded **S$_L$** and **Se$_L$** is 5.7kJ/mol, the ΔE_b between **S$_{1P}$** and **Se$_{1P}$** is only 2.2 kJ/mol. This can be explained in terms of the variation of the HB and ChB donor/acceptor capacity. It is most noteworthy the difference in the interaction energy value for the two different dimers, **S$_{3P}$** and **Se$_{3P}$,** where μ-μ is the dominant interaction probably due to the dipole moment of each molecule (μ) from **HSCN** (3.732D) to **HSeCN** (3.904D). This variation of μ is also evident in the rest of the **Se$_{nP}$** family. As occurred within thiocyanide complexes, intramolecular HB and μ-μ interactions dominate the complex bindings.

With the different intramolecular interactions for the S and Se dimers fully characterised, the study of the Te dimers was similarly performed by obtaining the different intramolecular noncovalent interactions. For this particular case and in terms of energy binding, **Te$_{1P}$** is not the most stable dimer of the family as for (**HSCN**)$_2$ and (**HSeCN**)$_2$ complexes, being complex **Te$_{2P}$** the most stable one. Furthermore, the three different complexes corresponding to the **Te$_{nP}$** disposition are very close in energy for this particular case. Even though these energy differences are very small, their implications on the interaction are huge and correlate with the μ of the **HTeCN** molecule (4.311D).

As observed in **Table 3**, the binding energies evolve with the size of the chalcogen, the larger the chalcogen, the stronger the interaction. In cases in which the chalcogen bond is present (**Y$_L$**, **Y$_{nN}$**) that evolution is due to the increase of the depth of the σ-hole. In case of **Y$_{nP}$**, those complexes are dominated by HBs and the E_b is mostly constant across the chalcogen atom type. What is more interesting is that those dimers involving μ-μ interactions (**Y$_{2P}$** and **Y$_{3P}$**) become more stable with the μ of the monomers involved. This has huge implications in molecular recognition since the design of structural patterns of moiety (such as -CN) which can perform μ-μ interactions can eventually

overcome, in theory, stronger interactions such as HB or chalcogen bonds.

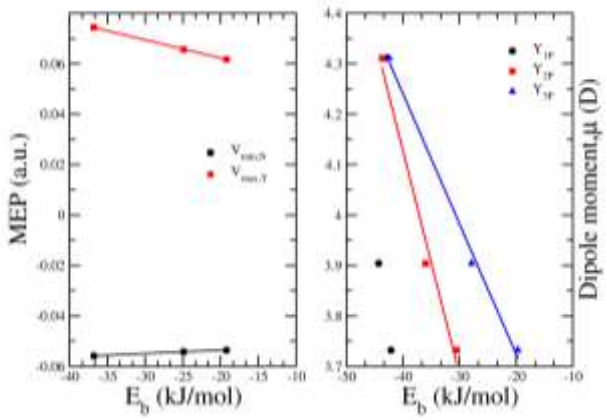

Figure 4. Correlation between MEP values and E_b for $\mathbf{Y_L}$ dimers (l.h.s.). Correlation between dipole moment values and E_b for $\mathbf{Y_{nP}}$ dimers (r.h.s.)

Binding energies E_b in dimers with $\mathbf{Y_L}$ disposition correlated with the **Y** σ-hole value ($V_{max,Y}$=0.047- 0.0007·E_b, R^2=0.999) and with the MEP minima value for the nitrogen lone pair (y= -0.0510+0.0001·E_b, R^2=0.995) which supports the chalcogen bond interaction. Besides, linear relationships have been found between the E_b and the value of the dipole moment for $\mathbf{Y_{2P}}$ (μ=2.3499-0.0444·E_b, R^2=0.982) and $\mathbf{Y_{3P}}$ (μ=3.2083-0.0258·E_b, R^2=0.995), while none has been found for $\mathbf{Y_{1P}}$. This again supports the evolution of the strength of the interactions with the dipole moment of the monomers (**Figure 4**).

Since it has been proved that the molecules under study play an important role in different biological functions, the solvent effect on the binding energies has been also explored by means of SMD model with water solvent. All the results have been gathered in **Table 4**. As a general trend, all complexes show a weakening on their E_b in solvent, however $\mathbf{Y_{2N}}$ and $\mathbf{Y_{3N}}$ complexes which exhibit more negative binding energies values in solvent than in gas phase. This may be due to the large dipole moment of the complexes which makes the molecule more sensitive to the solvent environment than Y_{nP} complexes. As observed, $\mathbf{Y_L}$ complexes have an increase of 33-49% on the E_b. $\mathbf{Y_{1P}}$ complexes seems to have a constant increase of 48.5-48.9% across the chalcogen type of atom. However, $\mathbf{Y_{2P}}$ and $\mathbf{Y_{3P}}$ exhibit the same trend observed in gas phase, the larger dipole moment, the larger variations of E_b: $\mathbf{S_{2P}}$ (+37.3%) < $\mathbf{Se_{2P}}$ (+44.9%) < $\mathbf{Te_{2P}}$ (+45.3%); $\mathbf{S_{3P}}$ (+18.4%) < $\mathbf{Se_{3P}}$ (+39.0%) < $\mathbf{Te_{3P}}$ (+47.2%).

Table 4. Binding energies, E_b^{SMD}(in kJ/mol) for all the dimers at the CCSD(T)/CBS computational level in SMD (water) solvent. Gas phase binding energies, E_b, in parenthesis for comparative purposes.

$(HSCN)_2$	E_b^{SMD} (E_b)	$(HSeCN)_2$	E_b^{SMD} (E_b)	$(HTeCN)_2$	E_b^{SMD} (E_b)
S_L	-11.6 (-19.2)	Se_L	-12.6 (-24.9)	Te_L	-24.7 (-36.8)
S_{1P}	-21.7 (-42.1)	Se_{1P}	-22.6 (-44.3)	Te_{1P*}	-
S_{2P}	-19.1 (-30.5)	Se_{2P}	-19.9 (-36.0)	Te_{2P}	-23.9 (-43.7)
S_{3P}	-16.0 (-19.7)	Se_{3P}	-17.0 (-27.9)	Te_{3P}	-22.4 (-42.4)
S_{1N}	-11.0 (-16.2)	Se_{1N*}	-	Te_{1N*}	-
S_{2N}	-	Se_{2N}	-15.8 (-15.9)	Te_{2N}	-24.7 (-21.7)
S_{3N}	-25.9 (-5.8)	Se_{3N}	-12.9 (-11.1)	Te_{3N}	-22.4 (-20.0)

**Geometry optimisations in solvent of Se_{1N}, Te_{1P} and Te_{1N} lead to a different dimer. Any attempt to obtain the same complex that in gas phase failed. For the sake of consistency, those complexes have been removed from the solvent table.*

Electronic properties (QTAIM)

The topological analysis of the electron density of the different dimers under study using Atoms in Molecules (QTAIM) indicates the existence of intermolecular bond critical point (BCP) between N···Y, N···H, Y···Y and Y···H atoms. Molecular graphs for all the complexes and electron density properties at the BCP have been summarised in **Tables S1** and **S2**. Values of the Laplacian ($\nabla^2\rho$) in **Table S2** indicates that all the interaction considered are within the closed shell range. In $\mathbf{Y_L}$ complexes, BCPs were found between N and the chalcogen atom Y. Values of the electron density at the BCP (ρ) indicate that those interactions correspond to weak interactions (chalcogen bonds), increasing ρ with the size of the chalcogen. In complexes $\mathbf{Y_{nP}}$, hydrogen bonds were also characterised with the corresponding BCP between the N and H atoms. The electron density of HBs BCP is larger than for the ChBs with the exception of **HTeCN** derivatives, which again indicates a preference for the ChB over HB. Another HB has also been found for $\mathbf{Y_{1N}}$ complexes, but as expected, lower values of ρ agreed with the strength of the interaction in comparison with $\mathbf{Y_{nP}}$ complexes. Finally, chalcogen···chalcogen interactions were found in $\mathbf{Y_{2N}}$ and $\mathbf{Y_{3N}}$ complexes, with ρ values evolving with the size of the chalcogen atom considered. Correlations between the intermolecular distance and both ρ and $\nabla^2\rho$ were explored. Due to the lack of points, no fair correlations were found for most of the interactions but for N···Y. In fact, in **Figure 5** (l.h.s) is observed that no correlations between ρ and N···Y distance was found. However, if only $\mathbf{Y_L}$ complexes are considered, it is observed an exponential relationship (y = 1127.1· $e^{-3.8257x}$, R^2= 0.958) which indicates that the other interactions are far more complicated that a simple chalcogen or hydrogen bond. However, Laplacian values (**Figure 5,** r.h.s) present an exponential correlation with the N···Y distance (y = 13.258 ·$e^{-1.8685\ x}$, R^2=0.909). This correlation is far better when only $\mathbf{Y_L}$ and $\mathbf{Y_{1N}}$ dimers are considered (y = 9.0268 ·$e^{-1.7305x}$, R^2=0.988). Similar exponential relationships were found between intermolecular distances *vs* ρ and intermolecular distances *vs* $\nabla^2\rho$ for similar non-covalent interactions.[36, 83-93]

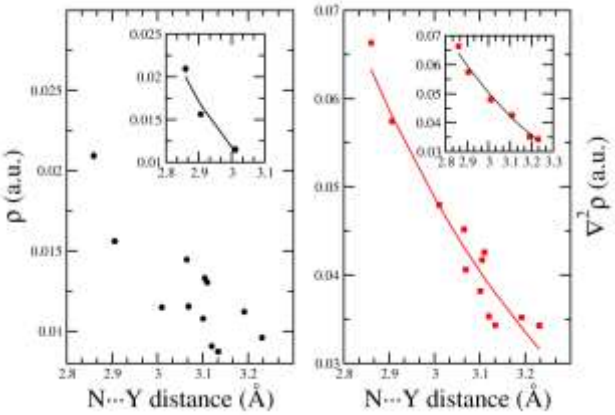

Figure 5. Correlation between the electron density at the BCP (ρ) and N···Y distance (l.h.s.). Correlation between the Laplacian at the BCP ($\nabla^2\rho$) and N···Y distance (r.h.s.).

NBO

The NBO analysis has been used to identify and characterised intermolecular charge transfer between occupied molecular orbitals and empty ones upon complexation. In **Table 5** the second order perturbation energies E(2) present in the complexes found are reported.

Among all the molecular interactions observed some of the largest contributions are coming from the HBs established between the lone pair of the N atom and S or Se empty σ bond (σ*H-Y) and found in complexes **Y_{1P}** and **Y_{2P}** (19.4 – 22.4 kJ/mol). An exception for this trend is the Te atom that contributes to the highest orbital interaction in the all series (35.7 kJ/mol) in complex **Y_L**. This corresponds to the only chalcogen bond interaction among all the different dimers where the lone pair of the N atom interacts with the σ–hole (σ*Y-C) of the chalcogen atom. In all the chalcogen bonds established in the series the orbital interaction decrease going from Te to S (Te > Se > S). This is independent from the fact that the chalcogen bond is exclusive (**Y_L** and **Y_{3N}**) or not (**Y_{1N}** and **Y_{2N}**) in forming the different dimers, and that the donation into the σ–hole is coming from a lone pair (N in **Y_L** or chalcogen atom in **Y_{2N}** and **Y_{3N}**) or from πCN (**Y_{1N}**). This is in agreement with the polarization of the different chalcogen atoms involved, S, Se and Te, and the depth of the σ–hole shown by MEP analysis. Orbital interactions that come either from the lone pair of N or from πCN into σ*Y-H found in complexes **Y_{2P}**, **Y_{3P}** are usually minimal (1.4 – 5.4 kJ/mol), except when Te is involved, where E(2) reaches 10.8 kJ/mol in complex **Y_{2P}**. The smallest contributions of the series come from the π-π interaction (πCN →*πCN) found in complexes **Y_{2P}** and **Y_{3P}** (2.0 – 2.9 kJ/mol). Also in this case, even if not as remarkable as for when a σ–hole is involved, a trend as Te > Se > S can be found.

Table 5. Second order orbital interaction energies, E(2), in kJ/mol for the all the dimers at the B3LYP/aug-cc-pVTZ computational level.

		E(2)		
	Orbital interaction	S	Se	Te
Y_L	$N_{lp} \rightarrow \sigma^*$Y-C	7.4	18.7	35.7
Y_{1P}	$N_{lp} \rightarrow \sigma^*$H-Y	20.6	22.4	18.5
Y_{2P}	$N_{lp} \rightarrow \sigma^*$H-Y	19.4	20.7	17.1
	$N_{lp} \rightarrow \sigma^*$Y-H	2.6	5.4	10.8
	πCN →*πCN	2.0	2.6	2.8
Y_{3P}	πCN →*πCN	2.0	2.6	2.9
	$N_{lp} \rightarrow \sigma^*$Y-H	2.4	4.5	8.6
	πCN → σ*Y-H	1.4	2.2	3.0
Y_{1N}	$Y_{lp} \rightarrow \sigma^*$H-Y	4.0	7.7	4.9
	$Y_{lp} \rightarrow$ *πCN	-	4.0	4.1
	πCN → σ*Y-C	2.3	5.1	8.9
Y_{2N}	πCN→ σ*H-Y	-	4.5	3.1
	$Y_{lp} \rightarrow \sigma^*$Y-C	-	6.1	22.0
Y_{3N}	$Y_{lp} \rightarrow \sigma^*$Y-C	4.0	9.2	21.4

Electron Density Shift Maps

In order to provide a visualisation of the changes on the electron density upon complexation, electron density shift (EDS) maps for (**HSCN**)$_2$ dimers have been plotted **Figure 6**. Yellow areas indicate regions of an increase of the electron density upon complexation, while purple ones are associated to areas with decreasing of the electron density. **S_L** dimer shows an increase in the region between S and N charactetistic of chalcogen bonds. Complex **S_{1N}** also presents a typical pattern for the ChB and HB with yellow areas closer to the electron donor and with purple areas (negatives) surrounded the acceptor. **S_{nP}** dimers show similar EDS plots than those found for previously reported cyanophosphines.[82] Also, it is observed that there is a slight reduction of the areas (both positive and negative) from **S_{1P}** to **S_{3P}**. This is in agreement with the weakening of the binding energy and the decrease of the importance of the electrostatic attractive term. This was observed for **S_{3N}** complex as well.

Figure 6. Electron Density Shifts at 0.0005 au for all the (**HSCN**)$_2$ dimers at MP2/aug-cc-pVTZ computational level. Yellow and purple areas represent positive (increase) and negative (decrease) electron density regions respectively.

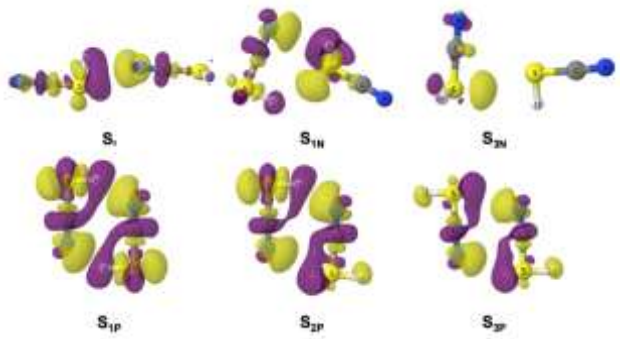

DFT-SAPT

Finally, the DFT-SAPT different energy terms have been summarised in **Table S3**. In **Figure 7**, the percentage of each attractive force has been plotted for each family of dimers, i.e. electrostatic term ($E_{el}^{(1)}$ blue), induction term ($E_i^{(2)}$ red) and dispersion term ($E_D^{(2)}$, green). As a general trend, the electrostatic term is the governing one, reaching up to 61% of the total attractive forces. The dispersion term, $E_D^{(2)}$, is the second most dominant attractive term, accounting for the 23%-69% of the total attractive term. In fact, **Y_{3N}** complexes shows $E_D^{(2)}$ values larger than $E_{el}^{(1)}$ ones. Same occurs for **Se_{2N}** and **Te_{2N}** complexes. As observed $E_i^{(2)}$ is the least important term with a contribution of 8-32%. It is most noteworthy that in the induction term seems to evolve with the chalcogen atom being for tellurium derivative complexes competitive with the dispersion one, particularly in **Te_L** and **Te_{3N}** complexes.

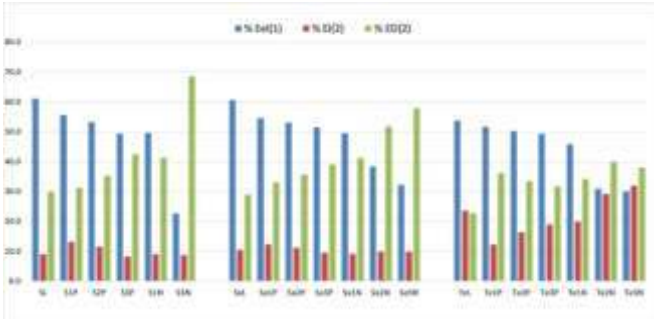

Figure 7. Graphical representation of the percentage of each attractive energy terms, $E_{el}^{(1)}$, $E_i^{(2)}$ and $E_D^{(2)}$ for all the dimers using the DFT-SAPT method.

Conclusions

In this manuscript the different non-covalent interactions established between (**HYCN**)$_2$ dimers (Y = S, Se and Te) have been studied at the MP2and CCSD(T)level of theory.

Firstly, the structure of the **HYCN** isolated monomers has been optimized and their structural parameters were found to be in good agreement with the experimental data present in the literature. Additionally, the molecular electrostatic potential (MEP) surface for each of the three monomers was calculated, in order to find maxima ($V_{max,X}$) and minima ($V_{min,X}$) values and assess the areas susceptible of nucleophilic and electrophilic attacks.

A total of 20 homodimers have ben been found upon complexation, 7 for both Se and Te dimers and only 6 for S atom. These complexes were categorized in terms of their geometrical disposition: complexes **Y$_L$** present monomers aligned head to tail; complexes **Y$_{nP}$** show both monomers with their Y-CN bond axis in parallel, and finally, complexes **Y$_{nN}$** show monomers Y-CN bond axis perpendicular one to each other.

Binding energies (E_b) in gas phase were found in the range of noncovalent interactions, from -5.8 to -44.3 kJ/mol. In case of those dimers dominated by HBs (**Y$_{nP}$**) the E_b are among the strongest of the all complexes and are more or less constant across the chalcogen atom type. What is more interesting is that those complexes involving μ-μ interactions (**Y$_{2P}$** and **Y$_{3P}$**) become more stable with the μ of the monomers involved. This trend is even more evident in solvent phase. For dimers in which ChBs are present (**Y$_L$**, **Y$_{nN}$**), when a comparison of the different binding energies across the chalcogen atoms is made, it is found that the larger the chalcogen, the stronger the interaction; according with the size of the chalcogen and due to the increase of the depth of the σ-hole. This can reach the point (especially for the Te series) in which the ChB found become competitive with μ-μ and HB interactions.

The characteristics of each interaction in the different types of dimers analysed by means of AIM have revealed the existence of intermolecular BCP between N···Y, N···H, Y···Y and Y···H atom. As a general trend, the electron density of HB BCPs is larger than the ChBs ones with the exception of **HTeCN** derivatives, which again indicates a preference for the ChB over HB. Once again, values of the electron density at the BCP (ρ) indicate that those interactions corresponding to weak interactions (chalcogen bonds), increase with the size of the chalcogen atom. Besides, Laplacian values ($\nabla^2\rho$) present an exponential correlation with the N···Y distance (R^2=0.909), which confirms the nature of the interactions found as noncovalent ones.

NBO and EDS analysis have been used to identify and provide a visualization on the changes of electron density upon complexation. According to NBO analysis HBs present among the largest E(2) orbital interaction energies, ranging from 17.1 to 22.4 kJ/mol. Once more, the exception is the Te atom that contributes to the highest orbital interaction in the all series (35.7 kJ/mol) with a ChB in complex **Y$_L$**.

Finally, SAPT-DFT has been used to evaluate the different terms of the interaction energy finding the highest contribution coming from the electrostatic term, $E_{el}^{(1)}$. The dispersion term, $E_D^{(2)}$, is the second most dominant attractive term, while the induction term, $E_i^{(2)}$, is the least important term. Interesting is the fact that for **Y$_{3N}$** complexes, $E_D^{(2)}$ is by far the governing one in case of S and Se, while for Te the induction term become very competitive, once again at support of the different behaviour of the cyano-tellurium series.

Computational details

The structures of the systems were optimized and characterized by means of MP2[94]/aug-cc-pVTZ[95, 96] calculations. Frequency calculations were carried out to confirm that the resulting structures correspond to energetic minima with no imaginary frequencies. All the optimizations have been performed in gas phase and in solvent (SMD, water). For Te atom aug-cc-pVTZ-PP pseudo potentials were used.

Furthermore, the binding energies were also estimated at the CCSD(T)/CBS (complete basis set) limit using the method of Helgaker et al.[97, 98] from the calculated interaction energies with the aug-cc-pVTZ and aug-cc-pVQZ basis sets:

$$E_X^{HF} = E_{CBS}^{HF} + A\, e^{-\alpha X} \quad (1)$$

$$E_X^{MP2} = E_{CBS}^{MP2} + B\, X^{-3} \quad (2)$$

$$E_{CBS}^{CCSD(T)} = E_{CBS}^{HF} + E_{CBS}^{MP2} + \left(E^{CCSD(T)} - E^{MP2}\right)_{AVTZ} \quad (3)$$

where E_X and E_{CBS} are the energies for the basis set with the largest angular momentum X and for the complete basis set, respectively. The CCSD(T)/CBS level can be attained via a separate extrapolation of the MP2 and higher-order correlation energies towards the basis-set limit (equation 3). Here, each of the components is differently sensitive to the AO basis set: the MP2 correlation energy is the more slowly converging, and the larger the basis set used in the extrapolation, the better. In our case we have used a two-point extrapolation scheme by using the aug-cc-pVTZ and the aug-cc-pVQZ basis sets. The third term, called the CCSD(T) correction term ($E^{CCSD(T)}$- E^{MP2}), is

determined as the difference between the CCSD(T) and MP2 energies and converges much faster than the MP2 correlation energy, the second term. The use of such a term is possible, because the MP2 and CCSD(T) energies converge with basis-set size in a very similar way; consequently, its difference is much less basis-set dependent and much smaller basis sets can be applied. In our case we have used the aug-cc-pVTZ basis set to compute the CCSD(T) correction. All the calculations were carried out with the Gaussian09 program.[99]

The molecular electrostatic potential (MEP) of the isolated monomers were calculated on the electron density isosurface of 0.001 au. This isosurface has been shown to resemble the van der Waals surface.[100] These calculations were carried out with the facilities of the Gaussian-09 program and the numerical results analysed using the Multiwfn[101] and plotted using Jmol.[102] Regions with negative MEP values are susceptible to interact with electron deficient moieties, such as HB donors, while positive regions can interact with electron rich areas.

The Atoms in Molecules (AIM) methodology[103, 104] was used to analyse the electron density of the systems with the AIMAll program.[105] The Natural Bond Orbital (NBO) method[106] was employed to evaluate atomic charges using the NBO-3 program, and to analyse charge-transfer interactions between occupied and unoccupied orbitals.

The intermolecular electron density shift (EDS) upon complexation was calculated using the fragmentation scheme proposed in ref. [107]and the Eq. 1.

$$EDS = \rho_{AB} - \rho_A - \rho_B \quad (1)$$

The different terms of the interaction energy were calculated with the DFT-SAPT methodology.[108, 109] The DFT-SAPT calculations were carried out using PBE0[107]/aug-cc-pVTZ/aug-cc-pVTZ-PP computational level.

When using the PBE0 functional, the asymptotic correction was included using the ionization potentials obtained at MP2/aug-cc-pVTZ computational level. All these calculations have been performed using the MOLPRO program. [110]

Acknowledgements

We thank the Irish Centre for High-End Computing (ICHEC), for the provision of computational facilities and support. Thanks are given to Prof. I. Alkorta for providing MOLPRO calculations.

Keywords: Non-covalent interaction •cyanides • chalcogen bonds • molecular recognition

References

[1] K. Müller-Dethlefs, P. Hobza *Chem. Rev.* **2000**, 100, 143-168.
[2] S. Scheiner *Acc. Chem. Res.* **2013**, 46, 280-288.
[3] B. A. Lodish H, Zipursky SL, et al. *Molecular Cell Biology.* . **2000**, 4th edition. New York: W. H. Freeman;.
[4] S. J. Grabowski *Chem. Rev.* **2011**, 111, 2597-2625.
[5] M. Nishio, M. Hirota, Y. Umezawa, The CH/π Interaction: Evidence, Nature, and Consequences, John Wiley & Sons, New York, **1998**.
[6] G. R. Desiraju, T. Steiner, The weak hydrogen bond, Oxford University Press, UK, **1999**.
[7] S. Grabowski, Hydrogen bonding - New insights, Springer, Dordrecht, The Netherlands, **2006**.
[8] P. Politzer, J. S. Murray, T. Clark *Phys. Chem. Chem. Phys.* **2013**, 15, 11178-11189.
[9] T. Clark *WIREs Comput. Mol. Sci.* **2013**, 3, 13-20.
[10] J. Murray, P. Lane, T. Clark, K. Riley, P. Politzer *J. Mol. Model.* **2012**, 18, 541-548.
[11] P. Politzer, J. S. Murray, T. Clark *Phys. Chem. Chem. Phys.* **2010**, 12, 7748-7757.
[12] T. Clark, M. Hennemann, J. Murray, P. Politzer *J. Mol. Model.* **2007**, 13, 291-296.
[13] I. Rozas, I. Alkorta, J. Elguero *Chem. Phys. Lett.* **1997**, 275, 423-428.
[14] I. Rozas, I. Alkorta, J. Elguero *J. Phys. Chem. A*. **1997**, 101, 4236-4244.
[15] A. Bauzá, T. J. Mooibroek, A. Frontera *Angew. Chem. Int. Ed.* **2013**, 52, 12317-12321.
[16] P. R. Varadwaj, A. Varadwaj, B.-Y. Jin *Phys. Chem. Chem. Phys.* **2014**, 16, 17238-17252.
[17] A. C. Legon *Phys. Chem. Chem. Phys.* **2017**, 19, 14884-14896.
[18] I. Alkorta, I. Rozas, J. Elguero *J. Phys. Chem. A*. **2001**, 105, 743-749.
[19] C. Trujillo, I. Alkorta, J. Elguero, G. Sánchez-Sanz *Molecules*. **2019**, 24.
[20] R. M. Minyaev, V. I. Minkin *Can. J. Chem.* **1998**, 76, 776-788.
[21] P. Sanz, M. Yáñez, O. Mó *New J. Chem.* **2002**, 26, 1747-1752.
[22] P. Sanz, O. Mó, M. Yañez *Phys. Chem. Chem. Phys.* **2003**, 5, 2942-2947.
[23] P. Sanz, M. Yáñez, O. Mó *Chem. Eur. J.* **2003**, 9, 4548-4555.
[24] G. Sánchez-Sanz, C. Trujillo, I. Alkorta, J. Elguero *ChemPhysChem*. **2012**, 13, 496-503.
[25] L. Azofra, I. Alkorta, S. Scheiner *Theor. Chem. Acc.* **2014**, 133, 1-8.
[26] K. W. Klinkhammer, P. Pyykko *Inorg. Chem.* **1995**, 34, 4134-4138.
[27] J. Moilanen, C. Ganesamoorthy, M. S. Balakrishna, H. M. Tuononen *Inorg. Chem.* **2009**, 48, 6740-6747.
[28] S. Zahn, R. Frank, E. Hey-Hawkins, B. Kirchner *Chem. Eur. J.* **2011**, 17, 6034-6038.
[29] S. Scheiner *J. Chem. Phys.* **2011**, 134, 094315-094319.
[30] S. Scheiner *J. Phys. Chem. A*. **2011**, 115, 11202-11209.
[31] U. Adhikari, S. Scheiner *J. Phys. Chem. A*. **2012**, 116, 3487-3497.
[32] A. Bauzá, D. Quiñonero, P. M. Deyà, A. Frontera *Phys. Chem. Chem. Phys.* **2012**, 14, 14061-14066.
[33] U. Adhikari, S. Scheiner *Chem. Phys. Lett.* **2012**, 536, 30-33.
[34] S. Scheiner *Comput. Theor. Chem.* **2012**, 998, 9-13.
[35] X.-L. An, R. Li, Q.-Z. Li, X.-F. Liu, W.-Z. Li, J.-B. Cheng *J. Mol. Model.* **2012**, 18, 1-8.
[36] G. Sánchez-Sanz, I. Alkorta, C. Trujillo, J. Elguero *ChemPhysChem*. **2013**, 14, 1656-1665.
[37] J. S. Murray, P. Lane, P. Politzer *Int. J. Quantum Chem*. **2007**, 107, 2286-2292.
[38] A. Mohajeri, A. H. Pakiari, N. Bagheri *Chem. Phys. Lett.* **2009**, 467, 393-397.
[39] P. Politzer, J. Murray, M. Concha *J. Mol. Model.* **2008**, 14, 659-665.
[40] W. Wang, B. Ji, Y. Zhang *J. Phys. Chem. A*. **2009**, 113, 8132-8135.
[41] T. Chivers, R. S. Laitinen *Chem. Soc. Rev.* **2015**, 44, 1725-1739.
[42] K. T. Mahmudov, M. N. Kopylovich, M. F. C. Guedes da Silva, A. J. L. Pombeiro *Dalton Trans.* **2017**, 46, 10121-10138.
[43] J. Fanfrlík, A. Přáda, Z. Padělková, A. Pecina, J. Macháček, M. Lepšík, J. Holub, A. Růžička, D. Hnyk, P. Hobza *Angew. Chem. Int. Ed.* **2014**, 53, 10139-10142.

[44] M. Iwaoka in *Chalcogen Bonds in Protein Architecture,* Springer International Publishing, Cham, **2015**, pp.265-289.
[45] B. R. Beno, K.-S. Yeung, M. D. Bartberger, L. D. Pennington, N. A. Meanwell *J. Med. Chem.* **2015**, 58, 4383-4438.
[46] A. Lange, M. Günther, F. M. Büttner, M. O. Zimmermann, J. Heidrich, S. Hennig, S. Zahn, C. Schall, A. Sievers-Engler, F. Ansideri, P. Koch, M. Laemmerhofer, T. Stehle, S. A. Laufer, F. M. Boeckler *J. Am. Chem. Soc.* **2015**, 137, 14640-14652.
[47] R. J. Fick, G. M. Kroner, B. Nepal, R. Magnani, S. Horowitz, R. L. Houtz, S. Scheiner, R. C. Trievel *ACS Chemical Biology*. **2016**, 11, 748-754.
[48] F. F. Fleming, L. Yao, P. C. Ravikumar, L. Funk, B. C. Shook *J. Med. Chem.* **2010**, 53, 7902-7917.
[49] N. Mast, W. Zheng, C. D. Stout, I. A. Pikuleva *J. Biol. Chem.* **2013**.
[50] J. George, V. L. Deringer, R. Dronskowski *J. Phys. Chem. A*. **2014**, 118, 3193-3200.
[51] J.-Y. Le Questel, M. Berthelot, C. Laurence *J. Phys. Org. Chem.* **2000**, 13, 347-358.
[52] A. Berteotti, F. Vacondio, A. Lodola, M. Bassi, C. Silva, M. Mor, A. Cavalli *ACS Medicinal Chemistry Letters*. **2014**, 5, 501-505.
[53] M. Feng, B. Tang, S. H. Liang, X. Jiang *Current topics in medicinal chemistry*. **2016**, 16, 1200-1216.
[54] J. D. Chandler, B. J. Day *Biochem. Pharmacol.* **2012**, 84, 1381-1387.
[55] Y. Xu, Sz, xe, S. p, Z. Lu *Proc. Nat. Aca. Sci. USA* **2009**, 106, 20515-20519.
[56] R. J. Capon, C. Skene, E. H.-T. Liu, E. Lacey, J. H. Gill, K. Heiland, T. Friedel *J. Nat. Prod.* **2004**, 67, 1277-1282.
[57] M. P. Fortes, P. B. N. da Silva, T. G. da Silva, T. S. Kaufman, G. C. G. Militão, C. C. Silveira *Eur. J. Med. Chem*. **2016**, 118, 21-26.
[58] E. Elhalem, B. N. Bailey, R. Docampo, I. Ujváry, S. H. Szajnman, J. B. Rodriguez *J. Med. Chem.* **2002**, 45, 3984-3999.
[59] G. G. Liñares, S. Gismondi, N. O. Codesido, S. N. J. Moreno, R. Docampo, J. B. Rodriguez *Bioorganic & medicinal chemistry letters*. **2007**, 17, 5068-5071.
[60] T. Castanheiro, J. Suffert, M. Donnard, M. Gulea *Chem. Soc. Rev.* **2016**, 45, 494-505.
[61] M. P. Rayman *The Lancet*. **2000**, 356, 233-241.
[62] C. A. Bayse, J. L. Brumaghim, Biochalcogen Chemistry: The Biological Chemistry of Sulfur, Selenium, and Tellurium, ACS Publications, Washinton, USA, **2013**.
[63] K. El-Bayoumy, P. Upadhyaya, Y.-H. Chae, O.-S. Sohn, C. V. Rao, E. Fiala, B. S. Reddy *J. Cell. Biochem.* **1995**, 59, 92-100.
[64] W. Ali, M. Álvarez-Pérez, M. A. Marć, N. Salardón-Jiménez, J. Handzlik, E. Domínguez-Álvarez *Current Pharmacology Reports*. **2018**, 4, 468-481.
[65] B. An, S. Zhang, J. Hu, T. Pan, L. Huang, J. C.-o. Tang, X. Li, A. S. C. Chan *Org. Biomol. Chem.* **2018**, 16, 4701-4714.
[66] P. M. Quatrin, D. F. Dalla Lana, L. C. G. Bazana, L. F. S. de Oliveira, M. Lettieri Teixeira, E. E. Silva, W. Lopes, R. F. S. Canto, G. P. Silveira, A. M. Fuentefria *New J. Chem.* **2019**, 43, 926-933.
[67] Y. Baquedano, V. Alcolea, M. Á. Toro, K. J. Gutiérrez, P. Nguewa, M. Font, E. Moreno, S. Espuelas, A. Jiménez-Ruiz, J. A. Palop, D. Plano, C. Sanmartín *Antimicrob. Agents Chemother.* **2016**, 60, 3802.
[68] D. Plano, Y. Baquedano, D. Moreno-Mateos, M. Font, A. Jiménez-Ruiz, J. A. Palop, C. Sanmartín *Eur. J. Med. Chem*. **2011**, 46, 3315-3323.
[69] R. Gowda, S. V. Madhunapantula, D. Desai, S. Amin, G. P. Robertson *Cancer Biology & Therapy*. **2012**, 13, 756-765.
[70] P. A. Grieco, Y. Yokoyama, E. Williams *The J.Org. Chem.*. **1978**, 43, 1283-1285.
[71] C. A. Bayse in *Modeling of Mechanisms of Selenium Bioactivity Using Density Functional Theory, Vol. 1152*, American Chemical Society, **2013**, pp.179-200.
[72] G. Jean-Claude *Curr. Org. Chem.* **2011**, 15, 1670-1687.
[73] T. Suzuki, H. Fujii, Y. Yamashita, C. Kabuto, S. Tanaka, M. Harasawa, T. Mukai, T. Miyashi *J. Am. Chem. Soc.* **1992**, 114, 3034-3043.
[74] O. Jeannin, H.-T. Huynh, A. M. S. Riel, M. Fourmigué *New J. Chem.* **2018**, 42, 10502-10509.
[75] A. Bundhun, M. D. Ramdany, J. S. Murray, P. Ramasami *Struct. Chem.* **2013**, 24, 2047-2057.
[76] M. D. Esrafili, S. Asadollahi *J. Sulfur Chem.* **2017**, 38, 83-97.

[77] Y. Zhang, W. Wang *Crystals*. **2018**, 8.
[78] S. Hauge, K. Marøy *Acta Chem. Scand.* **2018**, 46, 1166-1169.
[79] P. Du, N. E. B. Saidu, J. Intemann, C. Jacob, M. Montenarh *Biochimica et Biophysica Acta (BBA) - General Subjects*. **2014**, 1840, 1808-1816.
[80] R. L. O. R. Cunha, I. E. Gouvea, L. Juliano *Anais da Academia Brasileira de Ciências*. **2009**, 81, 393-407.
[81] C. Tapeinos, A. Pandit *Adv. Mater.* **2016**, 28, 5553-5585.
[82] G. Sánchez-Sanz, C. Trujillo, I. Alkorta, J. Elguero *Comput. Theor. Chem.* **2015**, 1053, 305-314.
[83] G. Sánchez-Sanz, I. Alkorta, J. Elguero *Mol. Phys.* **2011**, 109, 2543-2552.
[84] G. Sánchez-Sanz, C. Trujillo, M. Solimannejad, I. Alkorta, J. Elguero *Phys. Chem. Chem. Phys.* **2013**, 15, 14310-14318.
[85] G. Sánchez-Sanz, C. Trujillo, I. Alkorta, J. Elguero *Phys. Chem. Chem. Phys.* **2012**, 14, 9880-9889.
[86] O. Knop, R. J. Boyd, S. C. Choi *J. Am. Chem. Soc.* **1988**, 110, 7299-7301.
[87] I. Alkorta, L. Barrios, I. Rozas, J. Elguero *J. Mol. Struc. THEOCHEM*. **2000**, 496, 131-137.
[88] O. Knop, K. N. Rankin, R. J. Boyd *J. Phys. Chem. A*. **2001**, 105, 6552-6566.
[89] O. Knop, K. N. Rankin, R. J. Boyd *J. Phys. Chem. A*. **2002**, 107, 272-284.
[90] E. Espinosa, I. Alkorta, J. Elguero, E. Molins *J. Chem. Phys.* **2002**, 117, 5529-5542.
[91] I. Alkorta, J. Elguero *Struct. Chem.* **2004**, 15, 117-120.
[92] T. H. Tang, E. Deretey, S. J. Knak Jensen, I. G. Csizmadia *Eur. Phys. J. D.* **2006**, 37, 217-222.
[93] I. Mata, I. Alkorta, E. Molins, E. Espinosa *Chem. Eur. J.* **2010**, 16, 2442-2452.
[94] C. Møller, M. S. Plesset *Phys. Rev.* **1934**, 46, 618-622.
[95] D. E. Woon, T. H. Dunning *J. Chem. Phys.* **1995**, 103, 4572-4585.
[96] T. H. Dunning *J. Chem. Phys.* **1989**, 90, 1007-1023.
[97] A. Halkier, T. Helgaker, P. Jørgensen, W. Klopper, J. Olsen *Chem. Phys. Lett.* **1999**, 302, 437-446.
[98] A. Halkier, W. Klopper, T. Helgaker, P. Jørgensen, P. R. Taylor *J. Chem. Phys.* **1999**, 111, 9157-9167.
[99] M. J. Frisch, G. W. Trucks, H. B. Schlegel, G. E. Scuseria, M. A. Robb, J. R. Cheeseman, G. Scalmani, V. Barone, B. Mennucci, G. A. Petersson, H. Nakatsuji, M. Caricato, X. Li, H. P. Hratchian, A. F. Izmaylov, J. Bloino, G. Zheng, J. L. Sonnenberg, M. Hada, M. Ehara, K. Toyota, R. Fukuda, J. Hasegawa, M. Ishida, T. Nakajima, Y. Honda, O. Kitao, H. Nakai, T. Vreven, J. Montgomery, J. A., J. E. Peralta, F. Ogliaro, M. Bearpark, J. J. Heyd, E. Brothers, K. N. Kudin, V. N. Staroverov, R. Kobayashi, J. Normand, K. Raghavachari, A. Rendell, J. C. Burant, S. S. Iyengar, J. Tomasi, M. Cossi, N. Rega, N. J. Millam, M. Klene, J. E. Knox, J. B. Cross, V. Bakken, C. Adamo, J. Jaramillo, R. Gomperts, R. E. Stratmann, O. Yazyev, A. J. Austin, R. Cammi, C. Pomelli, J. W. Ochterski, R. L. Martin, K. Morokuma, V. G. Zakrzewski, G. A. Voth, P. Salvador, J. J. Dannenberg, S. Dapprich, A. D. Daniels, Ö. Farkas, J. B. Foresman, J. V. Ortiz, J. Cioslowski, D. J. Fox in Gaussian 16, Revision b1, Inc., City, **2016**
[100] R. F. W. Bader, M. T. Carroll, J. R. Cheeseman, C. Chang *J. Am. Chem. Soc.* **1987**, 109, 7968-7979.
[101] T. Lu, F. Chen *J. Comput. Chem.* **2012**, 33, 580-592.
[102] in Jmol: an open-source Java viewer for chemical structures in 3D. http://www.jmol.org/,
[103] R. F. W. Bader, Atoms in Molecules: A Quantum Theory, Clarendon Press, Oxford, **1990**.
[104] P. L. A. Popelier, Atoms In Molecules. An introduction, Prentice Hall, Harlow, England, **2000**.
[105] T. A. Keith in AIMAll, TK Gristmill Software (aim.tkgristmill.com), version 19.03.02. **2019**
[106] A. E. Reed, L. A. Curtiss, F. Weinhold *Chem. Rev.* **1988**, 88, 899-926.
[107] J. P. Perdew, K. Burke, M. Ernzerhof *Phys. Rev. Lett.* **1996**, 77, 3865-3868.
[108] A. J. Misquitta, R. Podeszwa, B. Jeziorski, K. Szalewicz *J. Chem. Phys.* **2005**, 123, 214103-214114.
[109] R. Moszynski *Mol. Phys.* **1996**, 88, 741-758.
[110] H.-J. Werner, P. J. Knowles, F. R. Manby, M. Schütz, P. Celani, G. Knizia, T. Korona, R. Lindh, A. Mitrushenkov, G. Rauhut, T. B. Adler, R. D. Amos, A. Bernhardsson, A. Berning, D. L. Cooper, M. J. O. Deegan, A. J. Dobbyn, F. Eckert,

E. Goll, C. Hampel, A. Hesselmann, G. Hetzer, T. Hrenar, G. Jansen, C. Köppl, Y. Liu, A. W. Lloyd, R. A. Mata, A. J. May, S. J. McNicholas, W. Meyer, M. E. Mura, A. Nicklass, P. Palmieri, K. Pflüger, R. Pitzer, M. Reiher, T. Shiozaki, H. Stoll, A. J. Stone, R. Tarroni, T. Thorsteinsson, M. Wang, A. Wolf in MOLPRO, version 2012.1, **2012**.

Entry for the Table of Contents

ARTICLE

In this manuscript the different noncovalent interactions established between $(HYCN)_2$ dimers (Y = S, Se and Te) have been studied The presence of hydrogen, chalcogen and dipole-dipole interactions was confirmed and their implications on molecular recognition were analysed.